Phosphatidylinositol monophosphate-binding interface in the oomycete RXLR effector AVR3a is required for its stability in host cells to modulate plant immunity

Takashi Yaeno[a], Hua Li[b], Angela Chaparro-Garcia[c], Sebastian Schornack[c], Seizo Koshiba[b,d], Satoru Watanabe[b], Takanori Kigawa[b,e], Sophien Kamoun[c], and Ken Shirasu[a,1]

[a]Plant Science Center and [b]Systems and Structural Biology Center, RIKEN, 1-7-22 Suehiro-cho, Tsurumi, Yokohama, Kanagawa, 230-0045 Japan; [c]The Sainsbury Laboratory, Norwich Research Park, Norwich NR4 7UH, United Kingdom; [d]Department of Supramolecular Biology, Graduate School of Nanobioscience, Yokohama City University, 1-7-29 Suehiro-cho, Tsurumi, Yokohama 230-0045, Japan; and [e]Department of Computational Intelligence and Systems Science, Interdisciplinary Graduate School of Science and Engineering, Tokyo Institute of Technology, 4259 Nagatsuta-cho, Midori-ku, Yokohama, 226-8502, Japan

Edited* by Brian J. Staskawicz, University of California, Berkeley, CA, and approved July 7, 2011 (received for review April 14, 2011)

The oomycete pathogen *Phytophthora infestans* causes potato late blight, one of the most economically damaging plant diseases worldwide. *P. infestans* produces AVR3a, an essential modular virulence effector with an N-terminal RXLR domain that is required for host-cell entry. In host cells, AVR3a stabilizes and inhibits the function of the E3 ubiquitin ligase CMPG1, a key factor in host immune responses including cell death triggered by the pathogen-derived elicitor protein INF1 elicitin. To elucidate the molecular basis of AVR3a effector function, we determined the structure of *Phytophthora capsici* AVR3a4, a close homolog of *P. infestans* AVR3a. Our structural and functional analyses reveal that the effector domain of AVR3a contains a conserved, positively charged patch and that this region, rather than the RXLR domain, is required for binding to phosphatidylinositol monophosphates (PIPs) in vitro. Mutations affecting PIP binding do not abolish AVR3a recognition by the resistance protein R3a but reduce its ability to suppress INF1-triggered cell death *in planta*. Similarly, stabilization of CMPG1 *in planta* is diminished by these mutations. The steady-state levels of non–PIP-binding mutant proteins *in planta* are reduced greatly, although these proteins are stable in vitro. Furthermore, overexpression of a phosphatidylinositol phosphate 5-kinase results in reduction of AVR3a levels *in planta*. Our results suggest that the PIP-binding ability of the AVR3a effector domain is essential for its accumulation inside host cells to suppress CMPG1-dependent immunity.

R protein | NMR | programmed cell death

The oomycete pathogen *Phytophthora infestans* is the causal agent of the late blight disease that led to the Irish potato famine in the late 1840s. Late blight still is one of the most serious biological threats to food security with yield losses caused by the pathogen in developing countries estimated to reach $6.7 billion annually (1). The *P. infestans* genome encodes a large repertoire of secreted disease effector proteins that are predicted to alter host physiology for successful colonization (2). After secretion, these effectors either accumulate in the plant intercellular space (apoplast) or translocate into host cells (3). Apoplastic effectors mainly are hydrolyzing enzymes, possibly functioning to degrade plant materials, or inhibitors, which block host defense-related enzymes. In contrast, RXLR and Crinkler (CRN) effectors function inside host cells to alter immune-signaling pathways (3, 4). The virulence mechanisms of these host-translocated effectors and the identity of the plant molecules they bind and target are poorly understood.

RXLR effectors are defined as modular secreted proteins that contain the characteristic amino-terminal motif Arg-X-Leu-Arg (where X is any amino acid) with rapidly evolving C-terminal effector domains (5, 6). The *P. infestans* genome is estimated to encode ~550 RXLR effectors, many more than in the other sequenced *Phytophthora* species, *P. sojae*, *P. ramorum*, and *P. capsici* (2, 7). Recent work reported that the N-terminal end of *P. sojae* Avr1b containing the RXLR motif is necessary and sufficient for both binding to phosphatidylinositol-3-phosphate (PI3P) and translocation into host cells (8, 9). Furthermore, a number of effectors from unrelated fungi were reported to contain motifs similar to RXLR and also mediated PI3P binding and cell entry. Based on these findings, Kale et al. (8) proposed that oomycete and fungal effector proteins bind to PI3P on the extracellular surface of host cells to facilitate entry into the host cytoplasm. However, this view has been challenged by a more recent report showing that the fungal effectors AvrM and AvrL567 do not require PI3P binding for cell entry (10).

P. infestans AVR3a originally was identified as an avirulence effector that is recognized by the corresponding resistance protein R3a in potato (11). Two major forms of naturally occurring *Avr3a* alleles are known: AVR3a^{K80I103} (AVR3a^{KI}) is recognized by R3a, and the other, AVR3a^{E80M103} (AVR3a^{EM}), evades recognition by the resistance protein (12). In the absence of R3a, both forms are able to suppress host cell death induced by the *P. infestans* elicitor protein INF1, although AVR3a^{KI} exhibits stronger inhibition activity (12). The ability of AVR3a to suppress INF1-induced cell death is abolished by the deletion of the C-terminal tyrosine (AVR3a^{Y147del}), but this deletion does not affect recognition by R3a, indicating that these two effector properties are mechanistically distinct (13). Indeed, AVR3a interacts with and stabilizes the host E3 ubiquitin ligase CMPG1 that mediates INF1-induced cell death but not R3a-triggered cell death (14–16). Consistently, the AVR3a^{Y147del} mutant fails to bind and stabilize CMPG1 *in planta* (14).

To understand the molecular basis of AVR3a effector activities, we determined the NMR solution structure of AVR3a4, a close homolog of AVR3a and Avr1b, from the pepper and cucurbit pathogen *P. capsici*. The structural and functional analyses of these effectors indicated that the AVR3a effector domain contains a conserved, positively charged surface patch and that this region, but not the RXLR domain, is required for binding to phosphatidylinositol monophosphates (PIPs). The

Author contributions: T.Y., A.C.-G., S.S., S. Kamoun, and K.S. designed research; T.Y., H.L., A.C.-G., S.S., and S.W. performed research; T.Y., H.L., A.C.-G., S.S., S. Koshiba, S.W., T.K., S. Kamoun, and K.S. analyzed data; and T.Y., H.L., A.C.-G., S.S., S.W., T.K., S. Kamoun, and K.S. wrote the paper.

The authors declare no conflict of interest.

*This Direct Submission article had a prearranged editor.

Data deposition: The atomic coordinates have been deposited in the Protein Data Bank (ID: 2LC2), and the NMR chemical shifts have been deposited in the Biological Magnetic Resonance Bank (accession no. 17588).

See Commentary on page 14381.

[1]To whom correspondence should be addressed. E-mail: ken.shirasu@psc.riken.jp.

This article contains supporting information online at www.pnas.org/lookup/suppl/doi:10.1073/pnas.1106002108/-/DCSupplemental.

steady-state levels of the non–PIP-binding AVR3a mutant proteins were reduced greatly *in planta*, although these proteins were properly folded and stable in vitro and were recognized by R3a *in planta*. In addition, overexpression of a phosphatidylinositol phosphate 5-kinase (PIP5K) led to reduction of WT AVR3a *in planta*. Thus, our results strongly suggest that the PIP-binding ability of the effector domain of AVR3a is essential for its accumulation inside host cells where it is required to modulate CMPG1-dependent plant immunity. These results do not support a general role for the RXLR domain in PIP binding.

Results and Discussion

Structural and Modeling Analysis of AVR3a4 and AVR3a. To study how AVR3a functions, we performed NMR-based structure and modeling analyses. First, we tested the solubility of derivatives of AVR3a and three close homologs, AVR3a4 and AVR3a11 from *P. capsici* and Avr1b from *P. sojae*. Then we assessed the propensity of the proteins to fold in vitro by 2D ^{1}H-^{15}N heteronuclear single quantum coherence spectra. Of the tested proteins, matured AVR3a4 lacking the signal peptide (Asn22–Tyr122) was found to be the most soluble and best folded in solution and therefore was used for further NMR structure analysis. The structural statistics and the NMR constraints of AVR3a4-derived peptide (Asn22–Tyr122) are summarized in Table S1. The effector domain (Gly59–Tyr122) formed a bundle of four α-helices (α1, Phe60–Ala75; α2, Lys79–Lys90; α3, Leu94–Phe100; α4, Asp110–Asp121) (Fig. 1 *A* and *B*), whereas the N-terminal region including the RXLR domain (Asn22–Arg58) was disordered. The rmsd for the helical regions of the effector domain are 0.36 Å for the backbone atoms and 0.83 Å for the heavy atoms. Based on the highly conserved sequences between AVR3a4 and AVR3a (Fig. 1*A*), a 3D structure of the AVR3a effector domain was built using homology modeling techniques (Fig. 1*C*). The modeled structure of the AVR3a effector domain (Ala77–Tyr147) also comprised four α-helices (α1, Thr79–Gly93; α2, Leu97–Asn107; α3, Leu112–Lys120; α4, Asn132–Leu142). Using the AVR3a structural model, we mapped Lys80 and Ile103, the key amino acids for recognition by R3a, on the N terminus of the α1 helix and the middle of the α2 helix, respectively (Fig. 1*D*). In addition, amino acid residues whose substitution in AVR3a^{EM} can regain R3a recognition were mapped on the exposed surface (Fig. S1*A*) (13). In contrast, most amino acids responsible for loss-of-function alleles were buried inside the helix bundle maintained by the interaction between W105 and Y135 that defines the W and Y motifs postulated by Dou et al. (9) (Fig. S1 *B* and *C*). C-terminal Tyr147, which is necessary for interaction with the E3 ubiquitin ligase CMPG1 and for suppression of INF1-induced cell death (14), was on a prominent flexible portion away from the putative R3a-recognition region of the other surface, suggesting that recognition regions for R3a and CMPG1 are physically distinct (Fig. 1*D*). However, because Y147 was on the flexible tail, it still is possible that Tyr147 may communicate with Lys80 and Ile103, which are required for suppression of INF1-induced cell death (12).

Mapping of the surface-charge distributions of AVR3a and AVR3a4 indicated that both proteins contain a patch of positively charged amino acids on one face and that these amino acids are derived mainly from the α1 helix (Fig. 1 *E* and *F*). Indeed, the positively charged amino acids Arg81, Lys85, Lys86, and Lys89 are conserved completely among all the homologs (Fig. 1*A*), indicating that this surface is likely to be important for function. A similar case was reported for the epsin N-terminal homology domain, which contains a conserved positively charged area on the bundle of four α-helices important for binding to phosphatidylinositol-4,5-bisphosphate (PI4,5P_2) (17). This finding is of particular interest because Avr1b previously was shown to bind to specific phospholipids (8).

AVR3a Binds to PIPs Via the Effector Domain, Not the RXLR Domain. To test whether AVR3a and AVR3a4 also bind to specific PIPs, a protein lipid overlay assay was performed with recombinant C-terminal GST-fusions of AVR3a (Asp23–Tyr147) and AVR3a4 (Asn22–Tyr122). AVR3a specifically bound to PI3P, phosphatidylinositol-4-phosphate (PI4P), and PI5P, but AVR3a4 did not bind to any of the PIPs (Fig. 2*A*). This result was surprising, because both recombinant AVR3 and AVR3a4 proteins possess an RXLR domain, which has been reported to function as a PIP-

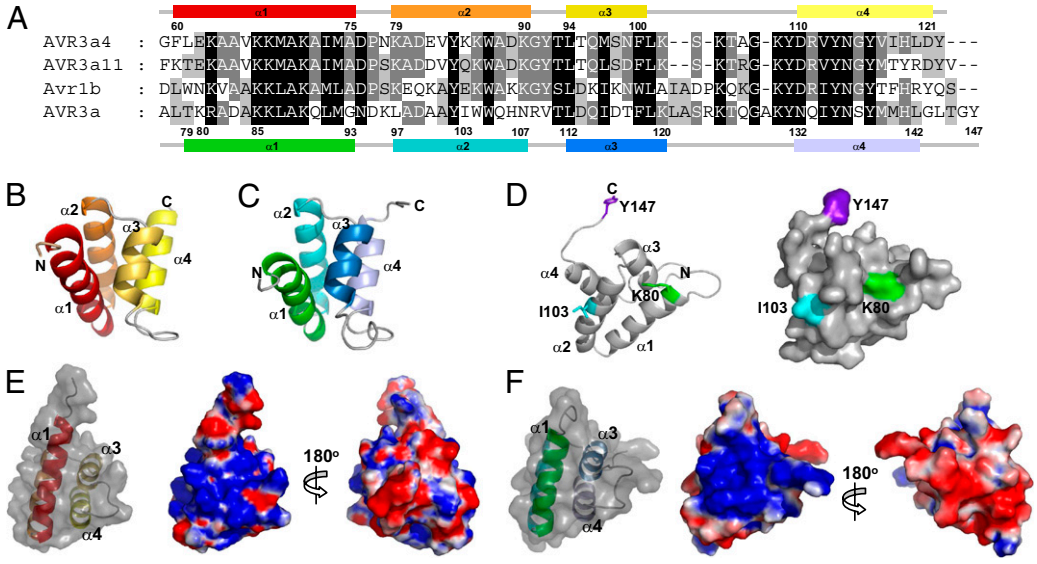

Fig. 1. Structural analysis of AVR3a4 and AVR3a. (*A*) Multiple sequence alignment of the effector domain of *Phytophthora* AVR3a and homologs. AVR3a4 and AVR3a11 are from *P. capsici*, Avr1b is from *P. sojae*, and AVR3a is from *P. infestans*. The helical regions and corresponding amino acid positions for AVR3a4 are shown above the alignment and for AVR3a are shown below the alignment. (*B* and *C*) Ribbon diagrams of the structures of (*B*) AVR3a4 and (*C*) AVR3a. (*D*) The important residues for R3a recognition (K80, green; I103, cyan) and INF1-induced cell death (Y147, purple) are mapped on the ribbon diagram (*Left*) and the surface structure (*Right*) of AVR3a. (*E* and *F*) Surface charge distribution of (*E*) AVR3a4 and (*F*) AVR3a. Electrostatic potential was calculated with PyMol (DeLano Scientific). Positively and negatively charged surfaces are shown in blue and red, respectively.

binding module (8). Instead, we noticed that the positively charged surface of the AVR3a4 effector domain is partially disrupted by negatively charged patches which presumably originate from the N-terminal half of the α1 helix (Glu62–Val66) (Fig. 1*E*), and we thought that this disruption might explain the differences in the PIP-binding activities of the two proteins. In fact, the fusion protein of the RXLR domain of AVR3a4 (Asn22–Arg58) with the effector domain of AVR3a (Ala60–Y147) bound to PIPs, whereas the chimera protein consisting of the RXLR domain and the α1 helix of AVR3a4 (Asn22–Met74) fused with the α2–α4 helices of AVR3a (Gly93–Tyr147) did not bind to any lipids (Fig. S2). These results do not support the notion that the RXLR domain of AVR3a4 contributes to PIP binding but suggest that the effector domain, in particular the α1 helix of AVR3a, is required for PIP binding. Consequently, we examined further whether the RXLR domain or the effector domain of AVR3a is required for binding to lipids by comparing the binding affinities of AVR3a variants to membranes spotted with serial dilutions of PIPs. An AVR3a derivative in which the RXLR motif RLLR (amino acids 44–47) was replaced by four Ala residues (AVR3a$^{RLLR/AAAA}$) still bound to PI3P, PI4P, and PI5P to the same extent as the WT (AVR3a^{KI}) (Fig. 2*B*). Furthermore, the C-terminal effector domain (Ala60–Tyr147) bound to PIPs, but the N-terminal region including the RXLR domain (Asp23–Arg59) did not (Fig. 2*B*). These results indicate that, unlike the previous report for Avr1b (8), AVR3a binds to PIPs via its C-terminal effector domain but not the N-terminal RXLR domain. In addition, the RXLR domain is not required for PIP binding.

Positively Charged Patch of the AVR3a Effector Domain Is Required for PIP Binding. To determine if the positively charged area of the effector domain is responsible for PIP binding, AVR3a mutants were generated by substituting Arg81, Lys85, Lys86, or Lys89 with the negatively charged amino acid glutamate (designated as AVR3a^{R81E}, AVR3a^{K85E}, AVR3a^{K86E}, or AVR3a^{K89E}, respectively; Fig. 2*C*). We found that AVR3a^{R81E} and AVR3a^{K86E} bound to PIPs with affinities similar to the WT protein. In contrast, the PIP-binding ability of AVR3a^{K85E} and AVR3a^{K89E} was lost or significantly reduced, respectively (Fig. 2*D*). In agreement with this result, the homology model of AVR3a^{K85E} showed that the positively charged patch was disturbed by Glu85 (Fig. S3). Taking these results together, we conclude that the positively charged patch of the AVR3a effector domain is required for binding to PIPs.

Given that *P. sojae* Avr1b is a close homolog of AVR3a, we explored the possibility that the effector domain of Avr1b also is involved in PIP binding. Molecular modeling of Avr1b revealed that, like AVR3a, the effector domain of Avr1b contains a positively charged surface patch in which the positively charged residues Lys79 and Lys83 correspond closely to Lys85 and Lys89 of AVR3a (Fig. 3*A*). Therefore, we re-examined the PIP-binding ability of Avr1b. As reported previously (8), WT Avr1b (Thr22–Ser138) bound to PIPs with a preference for PI3P (Fig. 3*B*). However, the PIP-binding ability of Avr1b^{K79E} was greatly reduced, and the Avr1b$^{K79E/K83E}$ double mutation almost completely abolished lipid binding (Fig. 3*B*). Additionally, two independent RXLR mutants, Avr1b$^{RFLR/AAAA}$ and Avr1b$^{RFLR/QFLR}$, bound to PIPs with the same affinity and specificity as WT (Fig. 3*B*). Together these results indicate that, as in AVR3a, the positively charged area formed by Lys79 and Lys83 in the effector domain, but not in the RXLR domain, is responsible for PIP binding by Avr1b. This result is markedly inconsistent with the previously reported topology of Avr1b lipid-binding activity (8).

PIP Binding Is Not Involved in Recognition of AVR3a by R3a. Coinfiltration of *Nicotiana benthamiana* leaves with mixtures of *Agrobacterium tumefaciens* strains expressing *Avr3a* and *R3a* results in the induction of R3a-dependent cell death (Fig. 4*A*) (11). The naturally occurring variant AVR3a^{EM}, which is not recognized by R3a, was able to bind to PIPs to a similar extent as AVR3a^{KI} (Figs. 2 and 4 *A* and *B*), implying that PIP binding and R3a recognition are distinct activities. Reciprocally, the AVR3a^{R81E}, AVR3a^{K85E}, AVR3a^{K86E}, and AVR3a^{K89E} mutants, in which the positively charged patch is disrupted, retained the ability to induce R3a-dependent cell death (Fig. 4 *A* and *B*),

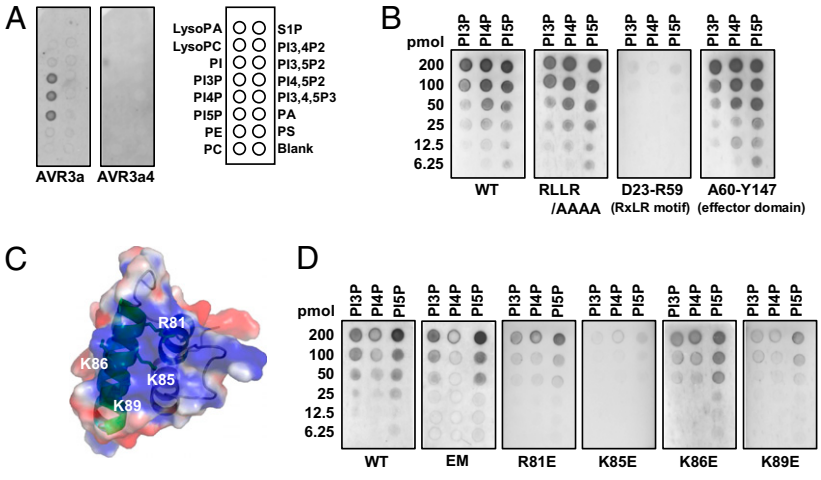

Fig. 2. The positively charged patch of the effector domain of AVR3a is required for binding to PIPs. (*A*) Protein lipid overlay assay of AVR3a and AVR3a4. One hundred picomoles of various lipids were spotted onto nitrocellulose membranes and incubated overnight with *E. coli*-expressed AVR3a-GST or AVR3a4-GST proteins at 4 °C. After rigorous washing, the bound proteins were detected using anti–GST-HRP antibodies. PA, phosphatidic acid; PC, phosphatidylcholine; PE, phosphatidylethanolamine; PI, phosphatidylinositol; PI3P, PI-3-phosphate; PI4P, PI-4-phosphate; PI5P, PI-5-phosphate; PI3,4P2, PI-3,4-biphosphate; PI3,5P2, PI-3,5-biphosphate; PI4,5P2, PI-4,5-biphosphate; PI3,4,5P3, PI-3,4,5-triphosphate; PS, phosphatidylserine; S1P, sphingosine-1-phosphate. (*B*) PIP binding of the RXLR mutant (RLLR/AAAA), the N-terminal region including the RXLR domain (23–59), and the effector domain (60–147) of AVR3a. Serial dilutions (200, 100, 50, 25, 12.5, and 6.25 pmol) of PI3P, PI4P, and PI5P were spotted onto nitrocellulose membranes. The protein lipid overlay assay was performed as in Fig. 2*A*. (*C*) Positions of positively charged amino acids Arg81, Lys85, Lys86, and Lys89 on the AVR3a structure. (*D*) PIP binding of AVR3a variants with mutations in the positively charged surface patch. The protein lipid overlay assay was performed as in Fig. 2*A*. EM, AVR3a^{EM}; WT, wild-type AVR3a^{KI}.

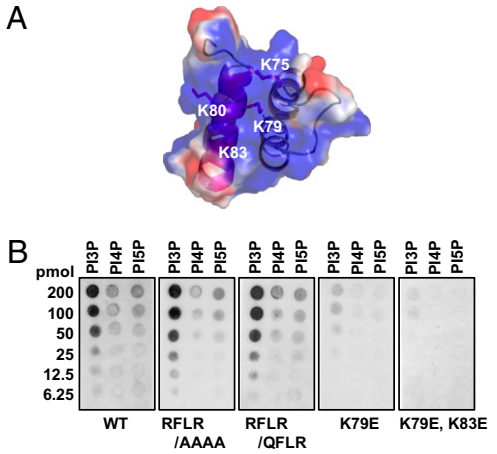

Fig. 3. A positively charged patch in the effector domain, but not the RXLR domain, of Avr1b is required for PIP binding. (*A*) Positions of positively charged amino acids Lys75, Lys79, Lys80, and Lys83 in the Avr1b structure. (*B*) PIP binding of the RXLR mutants Avr1b$^{RFLR/AAAA}$ and Avr1b$^{RFLR/QFLR}$ and AVR1b with mutations at the positively charged patch, Avr1b^{K79E}, and Avr1b$^{K79E,\ K83E}$. The lipid overlay assay was performed as in Fig. 2*A*.

confirming that PIP binding is not involved in recognition by R3a. Importantly, our results also indicate that these mutations do not affect the overall structure of AVR3a.

PIP Binding Is Required for Suppression of INF1-Induced Cell Death. Next, we examined whether mutations that reduce PIP binding also affect the suppression of INF1-induced cell death. In this assay, WT AVR3a or AVR3a mutants were transiently expressed in *N. benthamiana* by infiltration of recombinant *A. tumefaciens* strains into the leaves, followed by reinfiltration of the same area 1 d later with an *INF1*-expressing strain (Fig. 4 *C* and *D*) (12). AVR3a^{Y147del} was used as a positive control because it reduces the suppression activity of INF1-induced cell death to a degree similar to that observed in empty vector controls. Likewise, AVR3a^{K85E} and AVR3a^{K89E} failed to suppress INF1-induced cell death, suggesting that PIP binding is required for this suppression activity.

PIP Binding Is Necessary for Accumulation of CMPG1 and AVR3a *in Planta*. Because AVR3a is known to interact with and stabilize CMPG1 to suppress INF1-induced cell death (14), we tested whether mutations that reduce PIP binding also affect the steady-state levels of CMPG1 *in planta*. CMPG1 with an N-terminal 4× myc tag was coexpressed with N-terminal FLAG-tagged AVR3a mutants in *N. benthamiana* by agro infiltration. As previously reported, WT and AVR3a^{EM}, but not AVR3a^{Y147}, stabilized CMPG1 (Fig. 5*A*) and enabled its detection in immunoblots as two distinct migrating bands (14). In contrast, AVR3a^{K85E} was not able to stabilize CMPG1. In plants expressing AVR3a^{K89E}, the intensity of the upper CMPG1 band was reduced significantly, whereas the level of lower band remained similar to that observed for WT AVR3a (Fig. 5*A*). This result is consistent with inability of non–PIP-binding mutants to suppress INF1-induced cell death. Interestingly, the steady-state levels of AVR3a^{K85E} and AVR3a^{K89E} also were reduced to a certain extent *in planta,* with or without CMPG1 co-overexpression (Fig. 5 *A* and *B*). Importantly, purified *Escherichia coli*-expressed AVR3a^{K85E} and AVR3a^{K89E} did not aggregate and were stably soluble in vitro even after overnight incubation at room temperature (Fig. 5*B*). Furthermore, the circular dichroism spectra of the WT and AVR3a^{K85E} were nearly identical, suggesting that these proteins are folded properly (Fig. 5*C*). In the yeast two-hybrid experiments, both WT AVR3a and

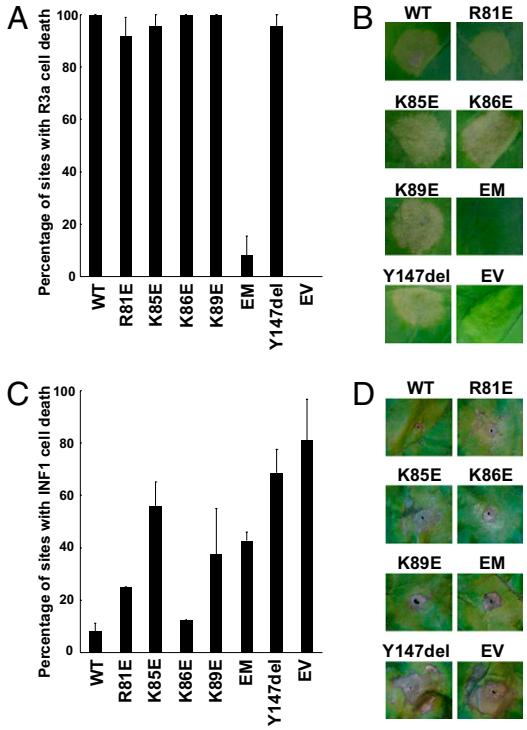

Fig. 4. PIP binding is not required for R3a-dependent recognition but is required for the suppression of INF1-induced cell death. (*A*) Percentage of R3a cell death induced by expression of AVR3a derivatives WT (AVR3a^{KI}), AVR3a^{R81E}, AVR3a^{K85E}, AVR3a^{K86E}, AVR3a^{K89E}, AVR3a^{EM}, and AVR3a^{Y147del} by *A. tumefaciens* infiltration. Cell death in *N. benthamiana* leaves was scored 5 d after infiltration. (*B*) Samples of infiltration sites coexpressing AVR3a derivatives with R3a. (*C*) Percentage of sites with INF1-induced cell death upon coexpression of INF1 with the AVR3 derivatives WT (AVR3a^{KI}), AVR3a^{R81E}, AVR3a^{K85E}, AVR3a^{K86E}, AVR3a^{K89E}, AVR3a^{EM}, and AVR3a^{Y147del}. Cell death was scored 5 d after infiltration with INF1. Error bars in *A* and *C* indicate SD of the means (n = 3). (*D*) Symptoms observed at infiltration sites coexpressing AVR3a derivatives with INF1.

AVR3a^{K85E} were able to interact with CMPG1, also suggesting that AVR3a^{K85E} is properly folded and that Lys85 is not required for its association with CMPG1 (Fig. 5*D*).

To test if the *in planta* reduction of AVR3a^{K85E} protein levels was caused by the introduction of a negative charge into the positively charged PIP-binding patch on the surface of the protein, we examined two other mutants, AVR3a^{K85A} and AVR3a^{K85G}, in which uncharged amino acids were substituted at position 85. As in AVR3a^{K85E}, the PIP-binding ability of AVR3a^{K85G} was greatly reduced. Surprisingly, however, AVR3a^{K85A} bound to PIPs with the same affinity as WT (Fig. 5*E*). Similarly, the steady-state levels of AVR3a^{K85G} were reduced compared with those of AVR3a^{K85E}, but AVR3a^{K85A} and WT were stable *in planta* (Fig. 5*F*). Furthermore, AVR3a^{K85G}, but not AVR3a^{K85A}, failed to suppress INF1-induced cell death (Fig. 5*G*). These results demonstrate that the PIP-binding ability of AVR3a is tightly correlated with its stability to suppress INF1-induced cell death *in planta*.

***PIP5K1* OX Suppresses Accumulation of AVR3a *in Planta*.** To study the relationship between PIPs and AVR3a *in planta*, we examined whether AVR3a was associated with membranes where PIPs are localized (18, 19). The accumulation of AVR3a was detected predominantly in the Nonidet P-40–treated extracts that contain a membrane marker H^+-ATPase, suggesting that AVR3a was present mainly in the membrane fraction (Fig. 6*A*). Because PI5PKs are known to be a modulator for phosphorylation states of membrane PIPs (20–25), we tested whether AVR3a levels

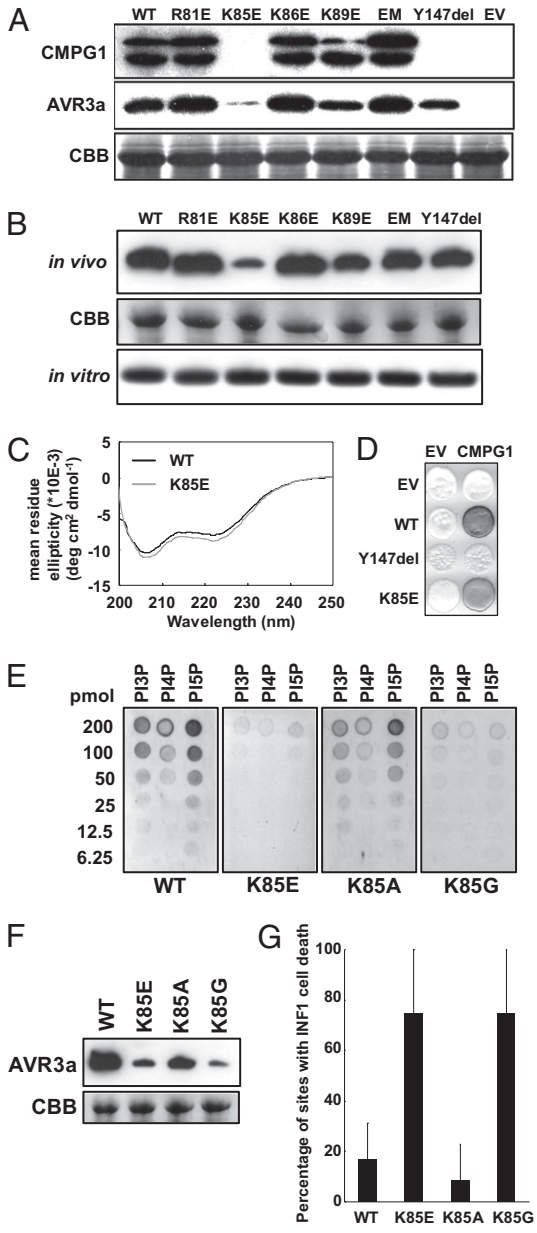

Fig. 5. PIP binding is required for the accumulation of CMPG1 and AVR3a *in planta*. (*A*) Immunoblots probed with anti-myc and anti-FLAG antibodies following coexpression of 4×-myc-CMPG1 and FLAG-AVR3a derivatives, respectively, in *N. benthamiana*. Protein loading is shown by Coomassie blue (CBB) staining. (*B*) Immunoblots probed with anti-FLAG antibody following expression of FLAG-AVR3a mutants in *N. benthamiana* (in vivo) and purified His-tagged AVR3a mutant proteins after incubation overnight at room temperature (in vitro). (*C*) Circular dichroism spectra of the purified His-tagged AVR3a proteins (WT, black; K85E, gray). (*D*) Interaction of AVR3a derivatives with CMPG1 in the yeast two-hybrid system. The expression of lacZ was monitored to check the interaction. (*E*) PIP binding of the Lys85 derivatives WT (AVR3a^{KI}), AVR3a^{K85E}, AVR3a^{K85A}, and AVR3a^{K85G}. The protein lipid overlay assay was performed as in Fig. 2*A*. (*F*) Immunoblots probed with anti-FLAG antibody following expression of FLAG-tagged Lys85 derivatives in *N. benthamiana*. (*G*) Percentage of sites with INF1-induced cell death upon coexpression of INF1 with Lys85 derivatives. Error bars indicate SD of the means (n = 3).

were affected by overexpression of PIP5K1, which phosphorylates PI3P and PI4P to PI3,4P2 and PI4,5P2, respectively (20). In *N. benthamiana* leaves coexpressing PIP5K1, the steady-state levels of AVR3a, but not plasma membrane-localized H$^+$-

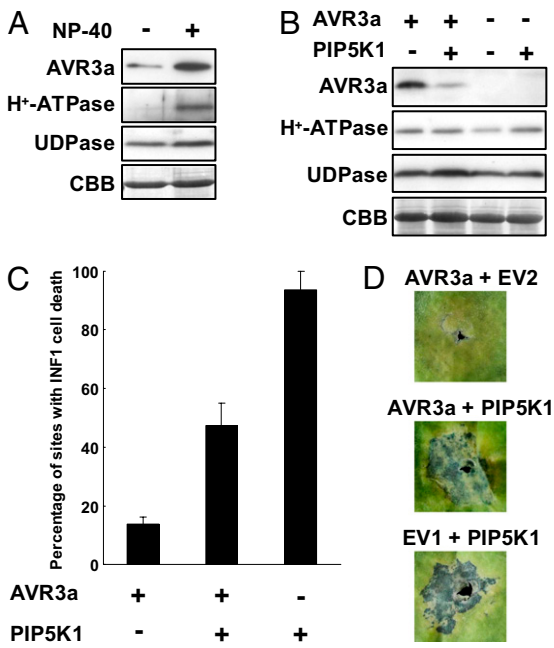

Fig. 6. *PIP5K1* OX suppresses the accumulation of AVR3a *in planta*. (*A*) Immunoblots probed with anti-FLAG antibody, anti–H$^+$-ATPase antibody, and anti-UDPase antibody, following expression of FLAG-AVR3a in *N. benthamiana*. The protein was extracted with or without Nonidet P-40 (NP-40). Protein loading is shown by Coomassie blue (CBB) staining. (*B*) Immunoblots probed with anti-FLAG antibody, anti–H$^+$-ATPase antibody, and anti-UDPase antibody, following expression of FLAG-AVR3a in *N. benthamiana* leaves overexpressing *PIP5K1*. (*C*) Percentage of sites with INF1-induced cell death upon coexpression of INF1 with AVR3a and PIP5K1. Cell death was scored 5 d after infiltration with INF1. Error bars indicate SD of the means (n = 3). (*D*) Symptoms observed at infiltration sites coexpressing INF1 with AVR3a and PIP5K1. *A. tumefaciens* strains carrying pGWB12 empty vector (EV1) or pEAQ-HT empty vector (EV2) were infiltrated as controls for AVR3a and PIP5K1, respectively.

ATPase and cytoplasmic UDPase, were reduced significantly (Fig. 6*B*). Consistently, AVR3a failed to suppress INF1-induced cell death in the PIP5K1-overexpressed leaves (Fig. 6 *C* and *D*). These results indicate further that PIP binding is crucial for AVR3a accumulation *in planta*.

Possible Roles of PIP Binding in AVR3a. Previous study has shown that the RXLR domain of AVR3a is sufficient for translocation of the effector into host cells (6). Our data presented here demonstrate that PIP binding is mediated not by the RXLR domain but by the positively charged surface patch of the C-terminal effector domain. Thus, our findings argue strongly against the proposed hypothesis for the general role of extracellular PI3P in RXLR-mediated effector entry (8). What is the role of AVR3a binding to PIPs? One possible function of PIP binding by AVR3a is to target CMPG1 effectively to endomembrane compartments within the host cytoplasm. Indeed, a recent report showed that CMPG1 was detectable in slow-moving vesicles in the host cytoplasm (15). Interestingly, when co-overexpressed with AVR3a in the absence of R3a, CMPG1 was found in the cytoplasm and nucleus (15). Furthermore, bimolecular fluorescence complementation experiments indicated that CMPG1 and AVR3a coexist mainly in the nucleus. We hypothesize that once PIP-bound AVR3a interacts with CMPG1, the AVR3a–CMPG1 complex may be released from vesicles and eventually accumulate in the nucleus where AVR3a stabilizes CMPG1 and alters its function. In the absence of PIP binding, AVR3a may become accessible to detection and removal by an

unknown host-intrinsic mechanism, thereby explaining the reduced stability of the non–PIP-binding mutants.

Our findings point to a PIP-binding module in the C termini of at least two *Phytophthora* RXLR effectors and suggest an important role for PIP-binding activity inside plant cells. Kale et al. (8) showed that several structurally unrelated fungal effectors bind PIPs, and recently Gan et al. (10) also showed that the C terminus of the flax rust effector AvrM strongly binds to phosphatidylinositol, PIPs, and phosphatidylserine. However, they ruled out a role for this activity in effector uptake into plant cells because the AvrM region that is sufficient for host translocation did not bind PIPs. Thus, lipid binding inside host cells may be a common feature of many oomycete and fungal effectors. In the future, understanding the molecular basis and the biological functions of effector lipid binding should help elucidate the virulence mechanisms of fungal and oomycete effectors.

Materials and Methods

Plasmid Construction. The procedures of the plasmid construction for NMR analysis, lipid-binding assay, and *in planta* expression are described in detail in *SI Materials and Methods*.

NMR Spectroscopy, Structure Determination, and Structural Analysis. The NMR spectra were recorded at 298 K on a Bruker AVANCE 700 MHz spectrometer equipped with a triple resonance cryoprobe. Details are given in *SI Materials and Methods*.

Protein Expression and Purification. *E. coli* strain BL21-AI (Invitrogen) was transformed with the pDEST17 or the pDEST24 vectors encoding *Avr3a* and its variants. Cultures were grown to an OD_{600} of 0.5 before induction of protein expression was induced by adding 0.2% arabinose and incubation at 28 °C for 3 h. Details of protein purification are provided in *SI Materials and Methods*.

Lipid-Binding Assay. Nitrocellulose membranes spotted with lipids were covered with protein solutions, and the lipid-protein interaction was detected as described in *SI Materials and Methods*.

Agroinfiltration Assay. *A. tumefaciens* GV3101 strains were grown in LB media supplemented with kanamycin at 50 μg/mL. Agroinfiltration experiments were performed on 3- to 5-wk-old *N. benthamiana* plants. Details of each agroinfiltration assay are provided in *SI Materials and Methods*.

Immunoblot Analyses. Immunoblot analyses were performed as described in *SI Materials and Methods*.

Circular Dichroism. The circular dichroism spectra of AVR3a and AVR3a^{K85E} were recorded at 4 °C on a J-820 Spectropolarimeter (JASCO) as described in *SI Materials and Methods*.

Yeast Two-Hybrid Assay. Details of the yeast two-hybrid assay are provided in *SI Materials and Methods*.

Note Added in Proof. While this article was being processed for publication, M. Banfield's group reported a similar structure of an AVR3a homolog, AVR3a11 (26).

ACKNOWLEDGMENTS. We thank Tsuyoshi Nakagawa for providing pGWB vectors; George P. Lomonossoff for providing pEAQ-HT vectors; Pamela Gan and Ivana Saska for critical reading of the manuscript; and Kaori Takizawa and Yoko Nagai for technical support. This work was supported by Grant-in-Aid for Scientific Research (KAKENHI) 19678001 (to K.S.), by the Gatsby Charitable Foundation (A.C.-G. and S. Kamoun), and by Deutsche Forschungsgemeinschaft Grant SCHO1347/1-1 (to S.S.).

1. Haverkort AJ, et al. (2008) Societal costs of late blight in potato and prospects of durable resistance through cisgenic modification. *Potato Res* 51:47–57.
2. Haas BJ, et al. (2009) Genome sequence and analysis of the Irish potato famine pathogen *Phytophthora infestans*. *Nature* 461:393–398.
3. Kamoun S (2006) A catalogue of the effector secretome of plant pathogenic oomycetes. *Annu Rev Phytopathol* 44:41–60.
4. Oliva R, et al. (2010) Recent developments in effector biology of filamentous plant pathogens. *Cell Microbiol* 12:705–715.
5. Birch PRJ, et al. (2008) Oomycete RXLR effectors: Delivery, functional redundancy and durable disease resistance. *Curr Opin Plant Biol* 11:373–379.
6. Whisson SC, et al. (2007) A translocation signal for delivery of oomycete effector proteins into host plant cells. *Nature* 450:115–118.
7. Lamour KH, Win J, Kamoun S (2007) Oomycete genomics: New insights and future directions. *FEMS Microbiol Lett* 274:1–8.
8. Kale SD, et al. (2010) External lipid PI3P mediates entry of eukaryotic pathogen effectors into plant and animal host cells. *Cell* 142:284–295.
9. Dou D, et al. (2008) RXLR-mediated entry of *Phytophthora sojae* effector Avr1b into soybean cells does not require pathogen-encoded machinery. *Plant Cell* 20: 1930–1947.
10. Gan PH, et al. (2010) Lipid binding activities of flax rust AvrM and AvrL567 effectors. *Plant Signal Behav* 5:1–4.
11. Armstrong MR, et al. (2005) An ancestral oomycete locus contains late blight avirulence gene *Avr3a*, encoding a protein that is recognized in the host cytoplasm. *Proc Natl Acad Sci USA* 102:7766–7771.
12. Bos JIB, et al. (2006) The C-terminal half of *Phytophthora infestans* RXLR effector AVR3a is sufficient to trigger R3a-mediated hypersensitivity and suppress INF1-induced cell death in *Nicotiana benthamiana*. *Plant J* 48:165–176.
13. Bos JIB, Chaparro-Garcia A, Quesada-Ocampo LM, McSpadden Gardener BB, Kamoun S (2009) Distinct amino acids of the *Phytophthora infestans* effector AVR3a condition activation of R3a hypersensitivity and suppression of cell death. *Mol Plant Microbe Interact* 22:269–281.
14. Bos JIB, et al. (2010) *Phytophthora infestans* effector AVR3a is essential for virulence and manipulates plant immunity by stabilizing host E3 ligase CMPG1. *Proc Natl Acad Sci USA* 107:9909–9914.
15. Gilroy EM, et al. (2011) CMPG1-dependent cell death follows perception of diverse pathogen elicitors at the host plasma membrane and is suppressed by *Phytophthora infestans* RXLR effector AVR3a. *New Phytol* 190:653–666.
16. González-Lamothe R, et al. (2006) The U-box protein CMPG1 is required for efficient activation of defense mechanisms triggered by multiple resistance genes in tobacco and tomato. *Plant Cell* 18:1067–1083.
17. Itoh T, et al. (2001) Role of the ENTH domain in phosphatidylinositol-4,5-bisphosphate binding and endocytosis. *Science* 291:1047–1051.
18. Vermeer JEM, et al. (2006) Visualization of PtdIns3P dynamics in living plant cells. *Plant J* 47:687–700.
19. Vermeer JEM, et al. (2009) Imaging phosphatidylinositol 4-phosphate dynamics in living plant cells. *Plant J* 57:356–372.
20. Westergren T, Dove SK, Sommarin M, Pical C (2001) AtPIP5K1, an Arabidopsis thaliana phosphatidylinositol phosphate kinase, synthesizes PtdIns(3,4)$P_{(2)}$ and PtdIns(4,5)$P_{(2)}$ in vitro and is inhibited by phosphorylation. *Biochem J* 359:583–589.
21. Lou Y, Gou JY, Xue HW (2007) PIP5K9, an *Arabidopsis* phosphatidylinositol monophosphate kinase, interacts with a cytosolic invertase to negatively regulate sugar-mediated root growth. *Plant Cell* 19:163–181.
22. Ischebeck T, Stenzel I, Heilmann I (2008) Type B phosphatidylinositol-4-phosphate 5-kinases mediate *Arabidopsis* and *Nicotiana tabacum* pollen tube growth by regulating apical pectin secretion. *Plant Cell* 20:3312–3330.
23. Kusano H, et al. (2008) The *Arabidopsis* phosphatidylinositol phosphate 5-kinase PIP5K3 is a key regulator of root hair tip growth. *Plant Cell* 20:367–380.
24. Stenzel I, et al. (2008) The type B phosphatidylinositol-4-phosphate 5-kinase 3 is essential for root hair formation in *Arabidopsis thaliana*. *Plant Cell* 20:124–141.
25. Zhao Y, et al. (2010) Phosphoinositides regulate clathrin-dependent endocytosis at the tip of pollen tubes in *Arabidopsis* and tobacco. *Plant Cell* 22:4031–4044.
26. Boutemy LS, et al. (2011) Structures of Phytophthora RXLR effector proteins: A conserved but adaptable fold underpins functional diversity. *J Biol Chem*, 101074/jbc. M111.262303.